Fatigue characterization of a polymer foam to use as a cancellous bone analog material in the assessment of orthopaedic devices

V. PALISSERY*, M. TAYLOR, M. BROWNE
Bioengineering Sciences Research Group, School of Engineering Sciences, University of Southampton, Highfield, Southampton, SOI 7 1BJ, UK
E-mail: vinu@soton.ac.uk

Analog materials are used as a substitute to cancellous bone for *in vitro* biomechanical tests due to their uniformity, consistency in properties and availability. To date, only the static material properties of these materials have been assessed, although they are often used in fatigue tests. Cancellous bone exhibits complex material behavior when subjected to fatigue loads, including modulus degradation, accumulation of permanent strain and increasing hysteresis. Analog materials should exhibit similar fatigue behavior to cancellous bone if they are to be used in cyclic loading tests.

In our study, a polymer foam (commercial name HEREX® C70.55) has been studied for its static and fatigue behavior and compared with that of cancellous bone. In compression, the foam exhibited qualitatively similar mechanical behavior, but the degree of modulus degradation and accumulation of permanent strain was lower than expected for cancellous bone. In general, the tensile properties of the foam were greater than found in compression, the opposite to the mechanical behavior of cancellous bone. The methodology employed here could form the basis of selecting suitable analog materials for cancellous bone in the future.

1. Introduction

The reported mechanical properties of cancellous bone show a wide variation depending on location, age and sex, in addition to the possible errors and variations in the measured values due to the use of different specimen geometries, test protocol and methods of data collection [1–10]. As a result, when assessing the mechanical performance of orthopedic devices, large numbers of bone samples are required to obtain statistically significant differences between designs. Availability, preparation and preservation of the bone samples make it a difficult material to work with. Alternative materials to cancellous bone, like polymer foams, for use in *in vitro* biomechanical tests [11–15] are attractive due to their consistent material properties, ease of use and availability. These materials are chosen based on a similar cellular structure and mechanical properties like strength, stiffness and strength/stiffness ratio falling in the same order as that of cancellous bone. To date, only the static properties of these materials have been evaluated and compared to the properties of cancellous bone [14, 15], even though they are used in fatigue tests.

Szivek [14, 15] reported the mechanical properties and preparation technique for two-component polyurethane foams and characterized the material for use in the study of acetabular subsidence based on the measurement of their elastic modulus, yield and compressive strength. By varying the ratio of the two components, resin and isocyanate, different foam densities were prepared for a range of mechanical properties. The foam structure and the mechanical behavior were studied for the different foam samples. The compressive modulus and strength were consistent, with a standard deviation of less than 10%, and the properties fell within the lower range of that observed for cancellous bone. The stress–strain curves had an initial linear phase and a plateau region after peaking. The average values of ultimate strength and modulus were in a range of 3.28–5.61 and 110.1–134 MPa, respectively for three different formulations of foam [15]. They suggested that synthetic foam was an attractive alternative to cancellous bone as a test substrate. Shirazi-adi [12] used a polyurethane foam as a substitute for tibial cancellous bone in an experimental and finite element comparison of various designs. They justified the use of polyurethane foam in place of cancellous bone in biomechanical testing due to its availability, homogeneity and relative control of the material properties and resemblance to cancellous bone in its porous structure and mechanical properties. Although this study included an experimental investiga-

*Author to whom all correspondence should be addressed.

tion of various fixation systems subjected to repetitive cyclic loads, only static tests were performed to characterize the foam. Commercially available synthetic bone models for the tibia and femur (e.g. bone models by Pacific Research Labs, Inc.) are used as a substitute to cadaver-bones in *in vitro* biomechanical tests. Rigid polyurethane foam is used as a substitute to cancellous bone in such models [11]. While composite femur models are used in cyclic loading tests [16], comparisons of the properties of the synthetic bone models and cadaveric bones under cyclic loads have not been performed. ASTM standards [17] give specifications for rigid polyurethane foam for use as a substitute material in orthopaedic tests. The specification provides mechanical properties, strength and modulus in shear and compression, for five different grades of foam in the solid form, but again the required fatigue behavior of the foam is not defined.

Qualitatively, trabecular bone behavior is considered to be similar to that of cortical bone. When subjected to fatigue loading cortical bone exhibits strength and modulus degradation and accumulation of strain/creep [18–20]. The number of cycles to failure showed power law relationship with the applied strain/normalized stress, where the relationships and patterns of modulus reduction were distinct in tension and compression. Although limited in number and restricted to compression testing only, *in vitro* studies have shown that cancellous bone exhibits complex fatigue behavior with degradation of strength, modulus and accumulation of strain/creep when subjected to cyclic loading [21–23]. Michel [23] studied the fatigue behavior of bovine trabecular bone. The number of cycles to failure (failure defined as 5% reduction in secant modulus) correlated with initial maximum global strain by a power law relationship. They observed a difference in modulus reduction with number of cycles for low and high cycles regimes. Bowman [21] studied the creep and fatigue characteristics of bovine proximal tibial cancellous bone. The amount of creep was large, often exceeding the initially applied strain. The progression of creep followed a distinct, primary, secondary and tertiary regimes. The parameter, normalized stress (stress normalized with secant modulus from the pre-conditioning test) was used to describe number of cycles to failure and steady state or secondary creep rate by power law relationships. They did not observe any distinct low–high cycle regimes. Haddock [22], conducted fatigue tests on cylindrical specimens of human vertebral cancellous bone. Modulus reduction at the time of failure was in the range of 25–55%, while strains at failure were in the range of 1.58–2.65%. The amount of modulus reduction and failure strains were related to the initial modulus and load levels.

Measurement of micromotion and migration of the implant-bone construct under cyclic loading is one of the major preclinical tests to assess the possible performance of the implant *in vivo* and to compare the performance of different implants. Synthetic bone models of the respective joints, made of substitute materials to bone, are used in many of these tests. The degree of micromotion (relative movement between implant and bone) and migration (permanent movement of implant from its initial position with respect to the bone) could be dependent on the behavior of the substrate materials under cyclic loading. Almost all the studies using substitute materials do not take account of the fact that the fatigue behavior of the substrate material can be different from the fatigue behavior of the cancellous bone. A similar structure and static behavior may not result in similar fatigue behavior of the two materials. In this context, the *in vitro* performance may be significantly different to the *in vivo* performance due to the fundamental differences in the fatigue behavior of a polymer foam and cancellous bone. The aim of this study is to characterize the fatigue behavior of an analog material HEREX C70.55, used in previous *in vitro* studies [13], and compare its behavior with that of cancellous bone.

2. Methods

Herex® C70.55 is a commercially available rigid, closed cell, cross-linked PVC foam with a high modulus and strength to weight ratio and is used as a core material for lightweight sandwich structures with applications in the fields of marine, road and rail and industrial parts. It has been previously used in *in vitro* experiments as an alternative to cancellous bone considering its cellular nature and modulus/strength ratio in compression falling into a similar range as cancellous bone [13]. All tests were performed on waisted cylindrical dumb bell shaped specimens. A waisted cylindrical shape will bias the failure of specimens towards a region of relatively high, uniform stress, where strain data are sampled, thus reducing the experimental artefacts to an extent [24]. The specimens were machined using a lathe. The waisted region of the specimens had a diameter of 15 mm and an approximate gauge length of 17 mm. The geometry of the specimen was identical for tension and compression tests. The specimen ends had a diameter of 20 mm and were 20 mm long and they were glued into metal end caps. This facilitated gripping of the specimen within the collets of the experimental jig without crushing the foam (Fig. 1(a)). The experiments were carried out on a computer-controlled Instron servo hydraulic load frame (Fig. 1(b)).

Five specimens each were tested in static tension and compression to assess the modulus and strength of the foam. All static tests were performed in strain control, with a crosshead movement rate of 0.1 mm/s, resulting in a strain rate of approximately 0.003/s within the gauge length. The load was recorded using a calibrated 1 kN capacity load cell and the deformation over gauge length was measured using an extensometer attached to the mid section of the specimens (Fig. 1(b)). Stress was calculated as the ratio of the load range and cross section area of the specimen within the gauge length. Strain was calculated as the ratio of elongation of extensometer from its initial position to the gauge length. Modulus was determined from the initial linear portion of stress–strain curve, by a linear fit of stress–strain curve between 0.1% and 0.4% strain [21, 24]. The ultimate strength in tension and compression were determined from the respective peak loads recorded in the tests.

The fatigue behavior of the foam was characterized in

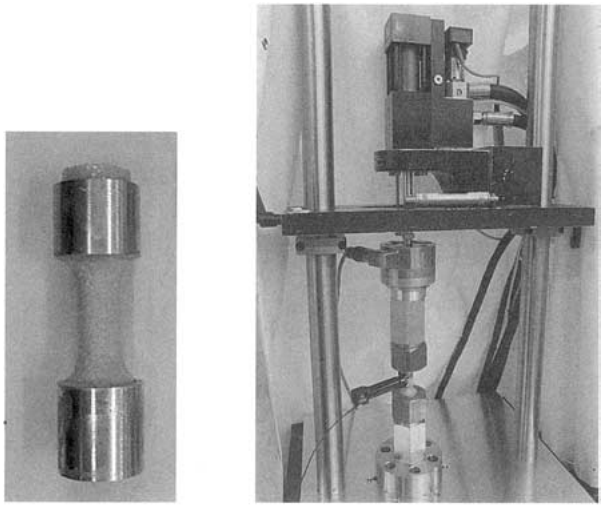

Figure 1 (a) Reduced section cylindrical specimens of the foam with metal end caps. (b) The experimental set-up; the extensometer, attached directly to the mid-section of the specimen, was used to measure the strain at various load cycles.

both tension and compression. Prior to the fatigue tests, all specimens were pre-conditioned, by applying 10 cycles at a lower stress level ($\approx$ 1/3 of ultimate strength) to determine the initial secant modulus in the elastic range, E_*. Fatigue tests, zero to compression and zero to tension were carried out at various stress ranges at a frequency of 2 Hz. The load and extensometer position data at minimum and maximum load amplitudes were collected at regular cycle intervals using a PC controlled data acquisition system.

Secant modulus (E) and accumulated strain (ε_{acc}) at various cycle intervals during the test were calculated using the following protocol (Fig. 2). The secant modulus at any cycle was defined as the ratio of stress range divided by the strain range. Accumulated strain at a particular load cycle, ε_{acc}, was defined as the translation of stress–strain curve along the strain axis with respect to the first cycle. The normalized modulus was used to represent the relative reduction in modulus at any given cycle and was defined as

$$\text{Normalized modulus} = \frac{E}{E_o} \quad (1)$$

where E is the secant modulus at any load cycle n and E_o is the secant modulus from the first cycle.

The parameter, normalized stress, which is defined as the ratio of applied stress (σ) to the initial secant modulus from the pre-conditioning test (E_*), is used as a variable to help describe the fatigue behavior. In order to assess the influence of the normalized stress, the data was analyzed in terms of the life fraction, which is defined as

$$\text{Life fraction} = n/N_f \quad (2)$$

where n is the current loading cycle and N_f is the number of loading cycles to failure. In the case of tensile fatigue tests the specimens failed by a total fracture at the midsection and N_f was taken as the number of cycles to fracture. For the specimens tested in compression, fracture of the samples rarely occurred. Therefore, failure was defined as the number of loading cycles to reach a 30% reduction in modulus compared to the initial secant modulus E_* at which point most of the specimens experienced a rapid increase in the deformation rate.

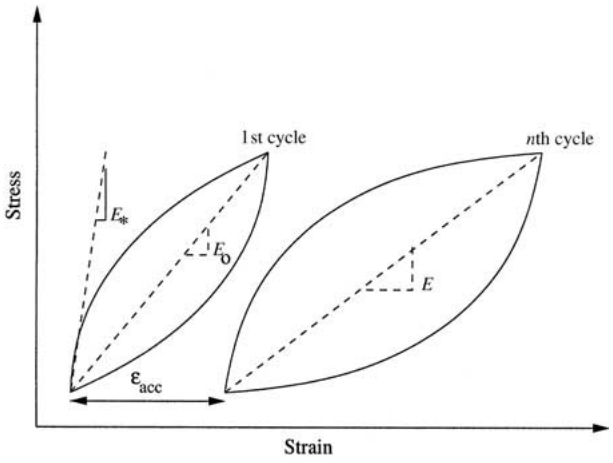

Figure 2 Schematic drawing of the method used to analyze the fatigue data. The accumulated/creep strain at any cycle n (ε_{acc}) is calculated as the translation of the stress-strain curve of the nth cycle along the strain axis with respect to the first cycle. For a given cycle, the secant modulus is defined as the stress range divided by the strain range, which is otherwise the slope of the line connecting the minimum and maximum stress values of that particular cycle. The initial secant modulus in the elastic range, determined from the pre-conditioning test is represented as E_*. The secant modulus from the first cycle is denoted as E_o and the secant modulus at any cycle n is represented as E.

3. Results

The static tests showed that for this particular foam, modulus and strength were higher in tension as compared to compression. Typical stress–strain curves of the material in tension and compression are shown in Fig. 3(a) and (b). The modulus of the material in tension and compression was 48.9 ± 3.3 and 39.6 ± 1.2 MPa, respectively. The strength of the material in tension and compression was 1.45 ± 0.09 and 0.64 ± 0.02 MPa respectively. In all cases, the standard deviation was less than 10% of the mean value. The modulus to strength ratio in tension and compression was ~ 34 and ~ 62, respectively.

A typical stress strain pattern under compressive cyclic loading is given in Fig. 4, which is qualitatively similar to that of cancellous bone. The maximum creep strain was less than the initial strain corresponding to the applied stress. Similar observations were recorded for tensile fatigue tests.

A summary of the results of the fatigue tests for tension and compression are given in Tables I and II, respectively.

3.1. The tensile fatigue behavior

The number of cycles to failure varied from 34 to 132252 for stress levels ranging from 93% to 46% of the ultimate strength. Fig. 5 shows logarithmic plot of normalized stress versus N_f. The number of cycles to failure, N_f, showed a power law relationship with normalized stress level as given below

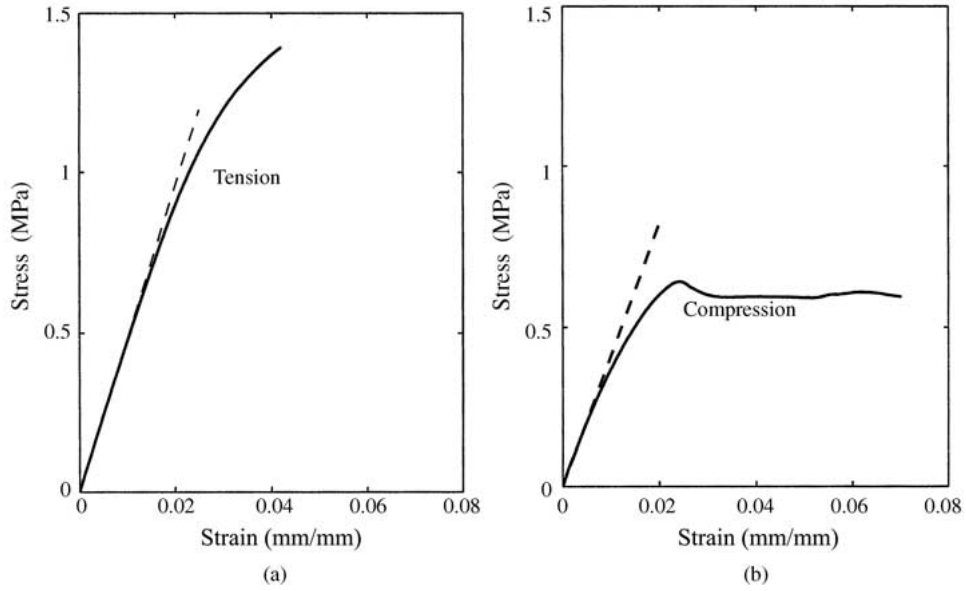

Figure 3 A typical stress strain pattern of the foam material under monotonic (a) tension and (b) compression. The modulus was calculated as the slope of the linear fit to the initial portion of the curves between strain of 0.1% and 0.4%.

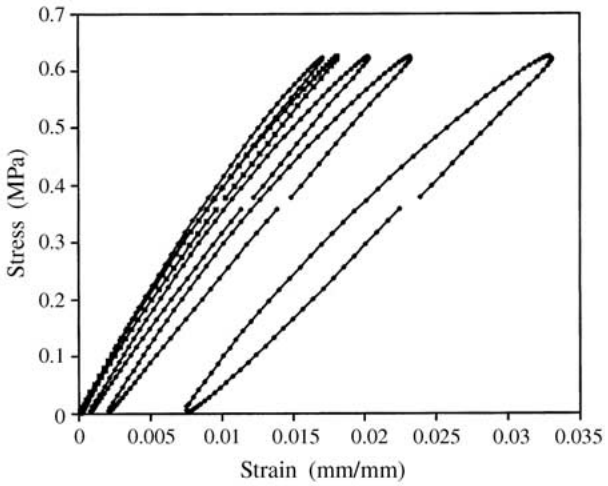

Figure 4 Typical stress strain pattern of the foam material under compressive cyclic load. As the number of cycles increased an increase in the hysteresis, decrease in the slope of the stress-strain curves and translation of the curves along the strain axis were observed.

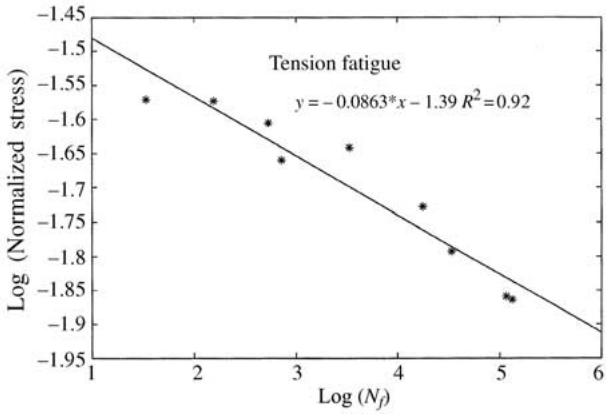

Figure 5 Normalized stress against life for tensile fatigue tests. A good linear relationship between the parameters exist in the logarithmic plot showing a power law relationship between the parameters.

$$N_f = 6.0 \times 10^{-17} (\sigma / E_*)^{-11.6} \quad R^2 = 0.92 \qquad (3)$$

The material exhibited modulus reduction and accumulation of strain (ε_{acc}) under cyclic loading. The variation of normalized modulus (E/E_o) and accumulation of permanent strain as a function of the life fraction (n/N_f) are shown in Fig. 6 and Fig. 7, respectively.

From Fig. 6, there appears to be two regimes for modulus degradation. A pattern of rapid reduction in the modulus at the very beginning of the tests was followed by a linear rate of modulus degradation at higher stress levels. At lower stress levels the modulus reduction pattern was linear and slow up to 90% of life, followed by a rapid reduction in modulus. The maximum amount of modulus reduction was 15% of the initial secant modulus for all the specimens. The accumulated strain pattern followed a classical creep curve, consisting of an initial rapid phase of deformation of decreasing rate, followed by a phase of linear deformation and a final phase of rapid deformation of increasing rate just prior to

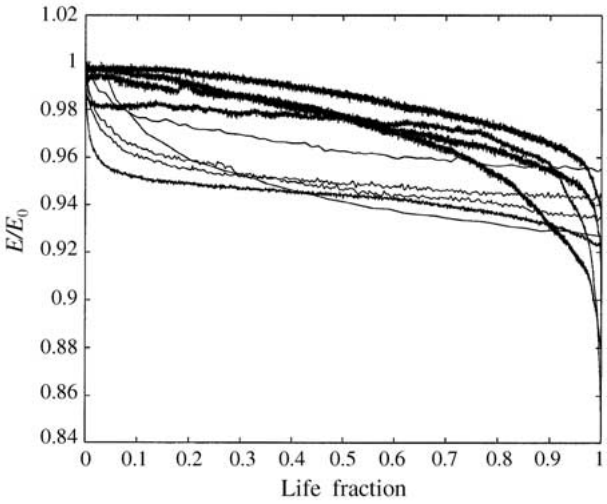

Figure 6 Normalized modulus against life fraction for tensile fatigue tests. At higher normalized stresses, a rapid reduction in the modulus at the very beginning of the fatigue life was followed by a gradual linear pattern of modulus reduction. At lower stress levels the modulus reduction was linear and slow up to 90% of fatigue life followed by a rapid reduction in modulus.

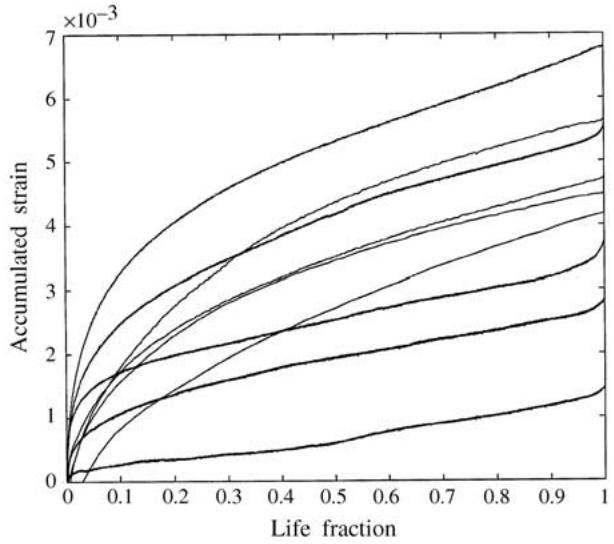

Figure 7 Accumulated strain against life fraction for tensile fatigue tests. The accumulated strain pattern followed a classical creep curve. The slope of the linear phase (steady state phase), identified between life fractions of 0.2 and 0.8 was related to the applied normalized stress levels by power law relationships.

failure. Visual inspection shows that the linear phase lies between life fractions of 0.2 and 0.8. At first inspection, there appeared to be no relationship between the degree of permanent strain accumulated during the test and the magnitude of the applied normalized stress. For each test, the constant rate of strain accumulation during the secondary stage was determined by a linear fit to the accumulated strain over the life fraction range from 0.2 to 0.8. The rate of strain accumulation during the second, steady state phase showed a power law relationship with the initial normalized stress σ/E_* as given below.

$$\frac{d\varepsilon_{\text{acc}}}{dN} = 4 \times 10^{13}(\sigma/E_*)^{11.6} \quad R^2 = 0.90 \qquad (4)$$

As the tests were carried out at a frequency of 2 Hz, steady state creep per second can be determined by multiplying the above relationship by 2.

3.2. Compressive fatigue behavior

In compression, the number of cycles to failure, N_{f}, showed a similar power law relationship with normalized stress level:

$$N_f = 2.2 \times 10^{-53}(\sigma/E_*)^{-29.4} \quad R^2 = 0.92 \qquad (5)$$

A log log plot of normalized stress against N_{f} is shown in Fig. 8.

For tests carried out at various stresses, falling in a range of 67–100% of the ultimate strength, the respective number of cycles to failure varied from 5 to 142380. Again, the material exhibited modulus reduction and accumulation of strain under compressive cyclic loading. The variation of normalized modulus (E/E_{o}) and accumulated strain with life fraction (n/N_{f}) are shown in Figs. 9 and 10 respectively. Due to lack of data points the results of the first three specimens from Table II were not included in the above plots. The pattern of modulus reduction was comparatively similar for all the specimens. There was a rapid modulus reduction for the initial

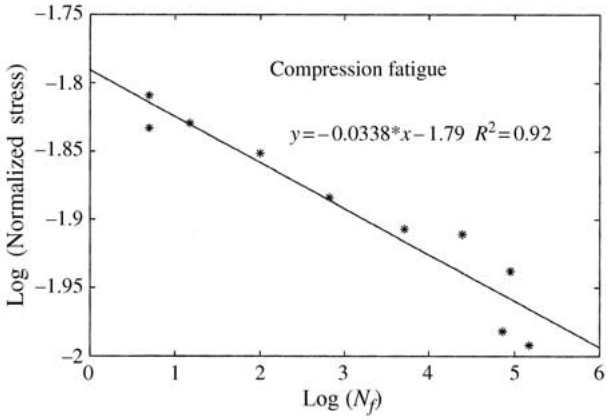

Figure 8 Normalized stress against life for compressive fatigue tests. A good linear relationship between the parameters exist in the logarithmic plot showing a power law relationship between the parameters.

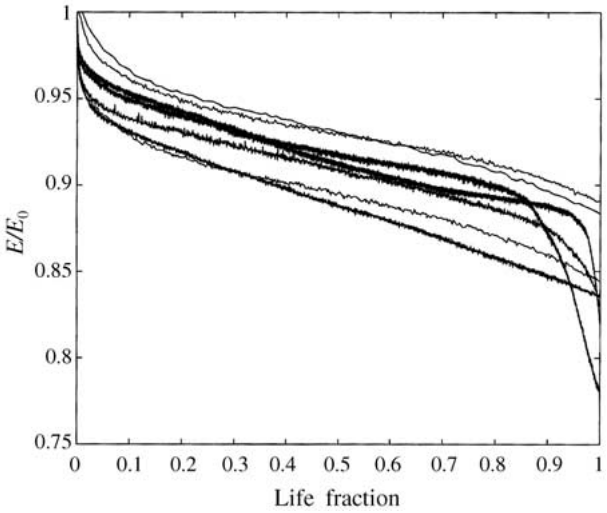

Figure 9 Normalized modulus against life fraction for compressive fatigue tests. The pattern of modulus reduction was similar for the range of normalized stress levels in which tests were carried out. A rapid modulus reduction in the initial 10% of life was followed by a linear region up to 90% of life and then a rapid phase.

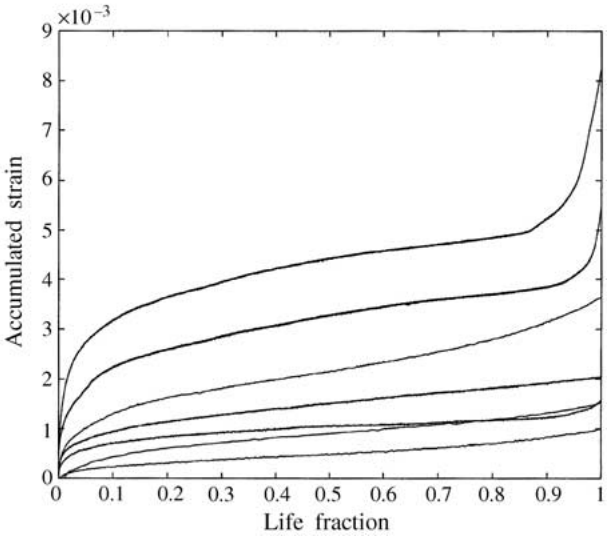

Figure 10 Accumulated strain against life fraction for compressive fatigue tests. In common with tensile fatigue tests, the accumulated strain pattern was similar to a standard creep curve and the rate of strain accumulation during the secondary phase showed a power law relationship with the normalized stress level.

TABLE I Tensile fatigue test results

Sl. No.	Stress, σ (MPa)	E_* (MPa)	E_o (MPa)	N_f
1	1.35	50.3	45.3	34
2	1.14	42.7	40.1	155
3	1.15	46.4	43.7	533
4	1.05	48.0	45.5	719
5	1.12	49.1	46.5	3381
6	0.93	49.7	49.4	17 780
7	0.81	50.2	50.7	34 033
8	0.73	52.8	53.3	1 15 700
9	0.67	49.0	48.8	1 32 252

TABLE II Compressive fatigue test results

Sl. No.	Stress, σ (MPa)	E_* (MPa)	E_o (MPa)	N_f
1	0.64	43.2	32.1	15
2	0.68	43.8	31.7	5
3	0.62	42.2	30.6	5
4	0.58	41.9	33.2	100
5	0.61	46.7	36.8	662
6	0.55	44.4	36.8	5140
7	0.49	39.9	33.4	24 490
8	0.46	44.1	37.2	72 429
9	0.51	44.2	37.8	89 524
10	0.43	42.2	37.8	1 47 710

10% of life followed by a linear region up to 90% of life and then a rapid phase. The tertiary phase was more distinct for lower stress levels. In common with the tensile tests, the accumulated strain pattern showed three stages and the rate of strain accumulation during the steady stage showed a power law relationship with σ/E_*. The strain curve over the life fraction range from 0.1 to 0.9 was used for the linear fit.

$$\frac{d\varepsilon_{acc}}{dN} = 7 \times 10^{31}(\sigma/E_*)^{20.1} \quad R^2 = 0.85 \qquad (6)$$

4. Discussion and conclusions

As a result of the wide variation in properties and the difficulties involved in working with cancellous bone, synthetic foams are widely used as an alternative in many *in vitro* biomechanical tests. These analog materials are chosen based on their porous structure, consistency in mechanical properties and their similarities to cancellous bone. It has to be noted that the comparisons of mechanical properties in many previous works were based on material behavior under monotonic loading and in many cases restricted only to compression. Although synthetic foams are used in tests involving cyclic loads, to date no studies have been found that compare the fatigue behavior of foam and cancellous bone. Cancellous bone shows complex material behavior when subjected to cyclic loads. In this respect, the present study suggests a methodology, which should be considered while choosing analog materials to cancellous bone.

Qualitatively, the static behavior of HEREX C®70.55 was similar to cancellous bone, though the material was stronger and stiffer in tension than compression. Strength and modulus values were consistent with a standard deviation less than 10%, and the values fall in the lowest range for cancellous bone [5, 9]. There is a consensus of opinion that tensile and compressive moduli of cancellous bone are equal. A linear relationship between tensile and compressive modulus is reported in some cases [25, 26]. However, there is a considerable debate as to whether the compressive strength is greater than, equal or less than the tensile strength [5, 26–28]. There is a general consensus of opinion that in general cancellous bone has greater strength in compression than in tension. If this is the case, then the foam used in this study is not a true representation of cancellous bone.

Under cyclic loading with a non-zero mean stress, cancellous bone exhibits significant material property degradation [21–23] with the modulus degrading by as much as 60% during fatigue tests and accumulated permanent strains that are of a similar order of magnitude as the initial applied strain. The number of cycles to failure and secondary state creep rate of cancellous bone under compressive fatigue loading has been shown to be strongly related to the normalized stress level by means of a power law relationship [21, 23].

The performance of the foam was qualitatively similar to the fatigue behavior of cancellous bone, particularly in compression, with the material exhibiting both modulus degradation and the accumulation of permanent strain. However, the amount of modulus reduction and creep for the material was less than that of cancellous bone. The maximum amount of creep, in both tension and compression, were less than 60% of initial applied strain and there was approximately a 30% reduction in modulus during a fatigue test. Generally there was more creep and stiffness reduction in compression than in tension for the analog material. Like bone, the foam showed power law relationships for life and secondary strain rate with normalized stress levels, and the relationships were distinct in tension and compression.

There are no clear explanations for the different failure modes in fatigue. Michel *et al*. [23] based on two different modes of failure at high and low cycle fatigue of cancellous bone suggested that crack growth or damage accumulation and creep as the dominant modes of failure at high and low cycle failure respectively. Bowman *et al*. [21] from the fatigue test results of cancellous bone observed no distinct low or high cycle regime and suggested that fatigue failure may be caused by a combination or interaction of damage accumulation and creep or by an additional creep buckling failure of the individual trabeculae.

Huang and Lin [29] derived the macrocrack growth rate of honeycombs and foams for three cases of microcrack propagation and low and high cycle fatigue (LCF and HCF) of the first unbroken cell walls ahead of the macrocrack tip using dimensional arguments. They arrived at a generalized expression for the microcrack growth irrespective of cell structure and cyclic stress intensity range. The constants in the derived expression were different for conditions of microcrack propagation and conditions of LCF and HCF; however, the constants depended on the cell size, relative density of the material

and the fatigue parameters of the solid cell wall materials.

Biomechanical tests using analog cancellous bone materials have been chosen to date based on their static properties and structure. With cancellous and cortical bone showing a distinct material behavior similar to a damaging material with considerable modulus reduction and accumulation of strain, analyzing the micromotion or migration results without a prior knowledge of the behavior of the substrate material can result in an interpretation different from reality depending on the qualitative and quantitative similarities of the material behavior to that of cancellous bone and on the purpose of the study.

The present study has shown that comparison of only static compression is not sufficient, as similar static behavior for two materials may not predict similar fatigue behavior. In this circumstance materials with a different behavior, either qualitatively or quantitatively to cancellous bone would result in an under estimation or over estimation of the mechanism under study. The study has demonstrated that though this analog material is a promising alternative to cancellous bone, the selection of analog material should be based not only on the similar static compression behavior, but also a similar compression/tension strength ratio and similar fatigue properties, particularly with respect to material property degradation. The methodology employed here could form a basis for the selection of a suitable analog *in vitro* test medium for assessing the performance of orthopedic devices.

Acknowledgments

The authors would like to thank Wright Medicals (UK) for their financial support.

References

1. J. C. BEHRENS, P. S. WALKER and H. SHOJI, *J. Biomech.* **7** (1974) 201.
2. T. D. BROWN and A. B. FERGUSON, JR, *Acta Orthop. Scan.* **51** (1980) 429.
3. R. HODGSKINSON and J. D. CURREY, *J. Mater. Sci. Mater. Med.* **3** (1992) 377.
4. I. HVID, *Dan. Med. Bull.* **35** (1988) 345.
5. T. M. KEAVENY and W. C. HAYES, *J. Biomech. Eng.* **115** (1993) 534.
6. T. M. KEAVENY, R. E. BORCHERS, L. J. GIBSON and W. C. HAYES, *J. Biomech.* **26** (1993) 991.
7. T. S. KELLER, *J. Biomech.* **27** (1994) 1159.
8. F. LINDE and I. HVID, *ibid.* **22** (1989) 485.
9. M. MARTENS, R. L. VAN AUDEKERCKE, P. DELPORT, P. de MEESTER and J. C. MULIER, *ibid.* **16** (1983) 971.
10. A. ODGAARD and F. LINDE, *ibid.* **24** (1991) 691.
11. L. CRISTOFOLINI, M. VICECONTI, A. CAPPELLO and A. TONI, *ibid.* **29** (1996) 525.
12. A. SHIRAZI-ADI, O. PATENAUDE, M. DAMARK and D. ZUKOR, *J. Biomech. Eng.* **123** (2001) 391.
13. J. A. Q. SIMOES, M. A. VAZ, J. A. G. CHOUSAL, M. TAYLOR and S. BLATCHER, in Proceedings of the International Conference on Advanced Technology in Experimental Mechanics, Wakayama, 1997, p. 423.
14. J. A. SZIVEK, M. THOMAS and J. B. BENJAMIN, *J. Appl. Biomater.* **4** (1993) 269.
15. J. A. SZIVEK, M. THOMAS and J. B. BENJAMIN, *ibid.* **6** (1995) 125.
16. S. A. MAHER, P. J. PRENDERGAST and C. G. LYONS, *Clin. Biomech.* **16** (2001) 307.
17. ASTM F1839-97 (1998) p. 1278.
18. W. E. CALER and D. R. CARTER, *J. Biomech.* **22** (1989) 625.
19. C. A. PATTIN, W. E. CALER and D. R. CARTER, *ibid.* **29** (1996) 69.
20. P. ZIOUPOS, X. T. WANG and J. D. CURREY, *Clin. Biomech.* **11** (1996) 365.
21. S. M. BOWMAN, X. E. GUO, D. W. CHENG, T. M. KEAVENY, L. J. GIBSON, W. C. HAYES and T. A. MC MOHAN, *J. Biomech. Eng.* **120** (1998) 647.
22. S. M. HADDOCK, O. C. YEH, P. V. MUMMANENI, W. S. ROSENBERG and T. M. KEAVENY, 46th Annual Meeting, Orthopaedic Research Society, Orlando, Florida, March 12–15, 2000.
23. M. C. MICHEL, X. E. GUO, L. J. GIBSON, T. A. MCMOHAN and W. C. HAYES, *J. Biomech.* **26** (1993) 453.
24. T. M. KEAVENY, X. E. GUO, E. F. WATCHEL, T. A. MCMOHAN and W. C. HAYES, *ibid.* **27** (1994) 1127.
25. R. B. ASHMAN, J. Y. RHO and C. H. TURNER, *ibid.* **22** (1989) 895.
26. L. ROHL, E. LARSEN, F. LINDE, A. ODGAARD and J. JORGENSEN, *ibid.* **24** (1991) 1143.
27. D. R. CARTER, G. H. SCHWAB and D. M. SPENGLER, *Acta Orthop. Scand.* **51** (1980) 733.
28. T. M. KEAVENY, E. F. WACHTEL, C. M. FORD and W. C. HAYES, *J. Biomech.* **27** (1994) 1137.
29. J. S. HUANG and J. Y. LIN, *Acta Mater.* **44** (1996) 289.

Received 12 November 2002
and accepted 9 July 2003